

# Spin Dependent Recombination Study of the Atomic-Scale Effects of Fluorine on the Negative Bias Temperature Instability

J.T. Ryan and P.M. Lenahan  
The Pennsylvania State University  
212 EES Bldg. University Park, PA 16802  
phone: 814-863-4630; e-mail: jtr16@psu.edu

A.T. Krishnan and S. Krishnan  
Texas Instruments  
Dallas, TX 75243

J.P. Campbell  
NIST  
Semiconductor Electronics Division  
Gaithersburg, MD 20899

**Abstract**— Recent work has shown that the negative bias temperature instability (NBTI) can be significantly suppressed through the incorporation of fluorine in the gate oxide of pure SiO<sub>2</sub> pMOSFETs. In this study, we use spin dependent recombination and standard gated diode current measurements to investigate the atomic-scale processes involved in fluorine's suppression of NBTI. We find that fluorine can effectively passivate Si/SiO<sub>2</sub> P<sub>b0</sub> center defect precursors, but is much less effective at passivating Si/SiO<sub>2</sub> P<sub>b1</sub> center defect precursors. Since these two defects have significantly different densities of states, our results may be useful in modeling NBTI response in fluorinated oxide devices. Our results also provide a fundamental explanation for the observation that fluorination has a strong effect on NBTI in “pure” SiO<sub>2</sub> MOS devices, but is ineffective at reducing NBTI in nitrided oxide devices.

**Keywords:** NBTI, Fluorine, Spin Dependent Recombination, Electron Spin Resonance

## I. INTRODUCTION

One of the most important reliability issues in modern MOS technology is the negative bias temperature instability (NBTI) [1-4]. NBTI is manifested as a threshold voltage shift and degradation of drive current in pMOSFETs due to the application of negative gate bias at elevated temperatures. Aggressive gate oxide scaling and the incorporation of nitrogen in the gate stack has exacerbated NBTI in recent years [1, 4]. Recent work suggests that NBTI may be somewhat suppressed by incorporating fluorine in the gate oxide [3, 5]. These observations are consistent with earlier suggestions that fluorine may passivate Si/SiO<sub>2</sub> dangling bond defects more effectively than hydrogen [6]. Other studies have also suggested that fluorine incorporation may be helpful in

reducing hot carrier damage [7, 8] and improving radiation hardness [9, 10]. Although progress has recently been made in identifying the atomic-scale defects responsible for NBTI in conventional SiO<sub>2</sub> and SiO<sub>x</sub>N<sub>y</sub> based devices [11, 12], not much is known about the atomic-scale effects of fluorine on NBTI. Our goal in this study is to begin to develop an atomic-scale understanding of the role fluorine plays in NBTI with the hope that this understanding will be helpful in developing processing techniques to ameliorate NBTI.

Electron spin resonance (ESR) is arguably the only technique with the analytical power and sensitivity to observe the atomic-scale defects responsible for MOS instability problems [13]. In earlier studies, the analytical power of ESR has been successfully utilized to study NBTI induced interface state generation in SiO<sub>2</sub> based large area MOS capacitor structures [11]. More recently, Campbell et al. utilized an extremely sensitive, electrically detected ESR technique called spin dependent recombination (SDR) to study NBTI induced defects in SiO<sub>2</sub> and SiO<sub>x</sub>N<sub>y</sub> MOSFETs [12]. SDR circumvents the sample requirements of conventional ESR which is limited to very large area capacitor structures and allows for the extraction of ESR information in fully processed transistors.

In this study, we employ SDR measurements to directly observe the atomic-scale effects of fluorine on NBTI response. Additional gated diode current measurements [14] (DC-IV) demonstrate a correlation between the SDR results and device parameter degradation (interface state generation).

## II. EXPERIMENTAL

We compare the effects of negative bias temperature stress (NBTS) on conventional pure SiO<sub>2</sub> devices and very similar

fluorinated SiO<sub>2</sub> devices. Both types of devices are large area (~40,000 μm<sup>2</sup>) pMOSFETs with identical gate oxide thickness (7.5 nm) and device geometry. Three differently processed sets of fluorinated devices were used.

SDR and DC-IV measurements were made before and after identical NBTS sequences (V<sub>g</sub> = -5.7 V at 140°C for 250,000 seconds). Following NBTS, all devices were subjected to a temperature quench step in which the gate bias stress was maintained as the device was brought to room temperature over approximately 4 minutes. We have found this to be fairly effective at “locking-in” NBTI-induced damage, rendering it observable in the SDR/DC-IV measurements [15]. SDR measurements were made at room temperature on a custom-built X-band spectrometer and were calibrated using a strong pitch spin standard.

### III. RESULTS AND DISCUSSION

Figures 1 and 2 illustrate representative pre- and post-NBTS DC-IV curves for the pure SiO<sub>2</sub> (Fig. 1) and a representative fluorinated SiO<sub>2</sub> (Fig. 2) device. The peak in the post-NBTS DC-IV curve, which scales with interface state density (D<sub>it</sub>), is nearly an order of magnitude smaller in the fluorinated case (Fig. 2). Following the analysis of Fitzgerald and Grove [14] and assuming a mean capture cross section of σ = 2 × 10<sup>-16</sup> cm<sup>2</sup>, D<sub>it</sub> values were extracted.

For pure SiO<sub>2</sub> (Fig. 1), D<sub>it</sub> = 7 × 10<sup>9</sup> cm<sup>-2</sup> eV<sup>-1</sup> for pre-NBTS and 5 × 10<sup>11</sup> cm<sup>-2</sup> eV<sup>-1</sup> for post-NBTS. For the representative fluorinated SiO<sub>2</sub> sample (Fig. 2), D<sub>it</sub> = 8 × 10<sup>9</sup> cm<sup>-2</sup> eV<sup>-1</sup> for pre-NBTS and 9 × 10<sup>10</sup> cm<sup>-2</sup> eV<sup>-1</sup> for post-NBTS. The reduction in post-NBTS D<sub>it</sub> of Fig. 2 (compared to the nearly identical pure SiO<sub>2</sub> sample) was observed in all three sets of fluorinated SiO<sub>2</sub> devices in our study. This is consistent with other reports indicating less NBTI damage in fluorinated SiO<sub>2</sub> devices [3, 5].

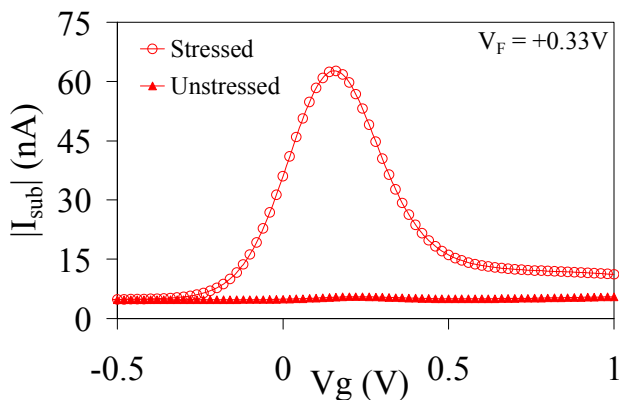


Fig. 1. Representative pre- and post-NBTS DC-IV curves for the pure SiO<sub>2</sub> devices.

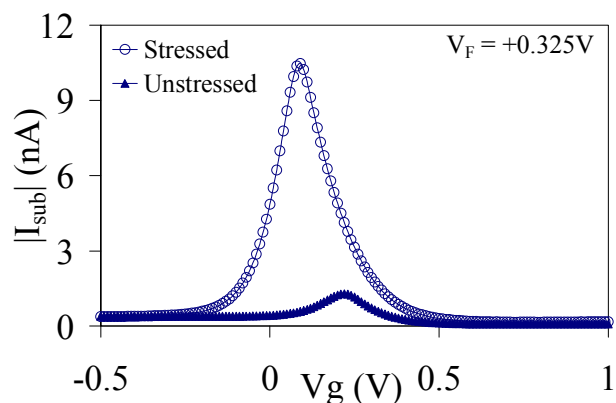


Fig. 2. Representative pre- and post-NBTS DC-IV curves for the fluorinated SiO<sub>2</sub> devices. Note the decreased amplitude of the peak compared to the pure SiO<sub>2</sub> curve of Fig. 1. The smaller post-NBTS D<sub>it</sub> for the fluorinated devices was consistently observed in our study.

Figures 3 (pure SiO<sub>2</sub>) and 4 (fluorinated SiO<sub>2</sub>) illustrate SDR traces of the two post-NBTS devices utilized in Figs. 1 and 2. In these traces the magnetic field is parallel to the [100] Si/SiO<sub>2</sub> interface normal. Pre-NBTS defect spectra were below the detection limit of the spectrometer. Note that in these figures, the spectrometer gain for the pure SiO<sub>2</sub> trace (Fig. 3) is much lower than the fluorinated SiO<sub>2</sub> trace (Fig. 4). Fig. 3 exhibits two somewhat overlapping signals with g values of 2.0057 and 2.0031 which are, respectively, due to Si/SiO<sub>2</sub> P<sub>b0</sub> and P<sub>b1</sub> centers [13, 16]. (The g is defined as g = hv/βH, where h is Planck’s constant, v is the microwave frequency, β is the Bohr magneton, and H is the magnetic field at resonance. The g depends on the defect’s structure and orientation with respect to the applied magnetic field; it is essentially a second rank tensor [17].) Note that Fig. 3 is representative of NBTI SDR results on many essentially pure SiO<sub>2</sub> pMOSFETs, as reported earlier [12]. The Fig. 4 trace exhibits a significantly different and much weaker single line spectrum with a g of 2.0026 which is consistent with a P<sub>b1</sub> center. Note also the somewhat broader width of the signal of Fig. 4. This may indicate the presence of nearby fluorine nuclei [17].

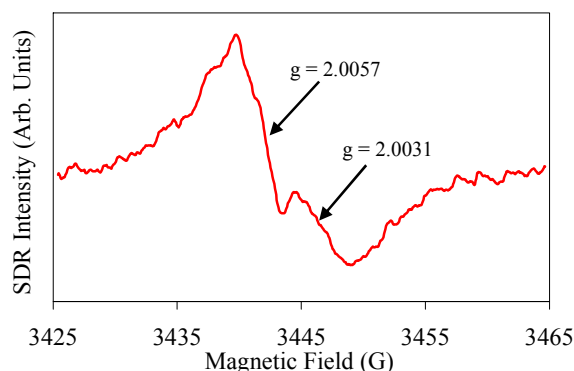


Fig. 3. Post-NBTS SDR traces for the pure SiO<sub>2</sub> device of Fig. 1. The two signals are due to P<sub>b0</sub> (g = 2.0057) and P<sub>b1</sub> (g = 2.0031) Si/SiO<sub>2</sub> interface defects. Note that this data is representative of NBTI SDR results on many essentially pure SiO<sub>2</sub> pMOSFETs, as reported earlier [12].

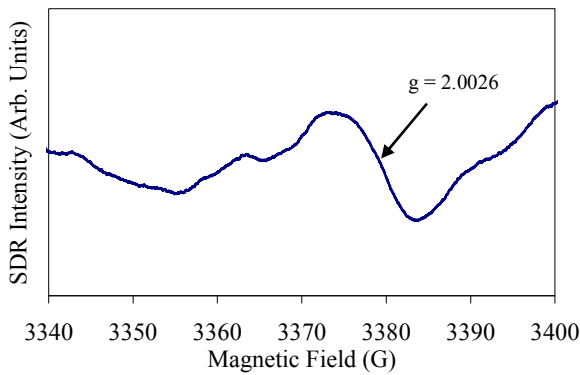


Fig. 4. Post-NBTS SDR traces for the fluorinated SiO<sub>2</sub> device of Fig. 2. The signal is consistent with a P<sub>b1</sub> Si/SiO<sub>2</sub> interface defect. The gain is much higher and the sweep width is greater to compensate for the much weaker and somewhat broadened signal.

Although the device of Fig. 4 is very similar structurally and was stressed identically as the pure SiO<sub>2</sub> device of figure 3, their NBTI response is very different. For the case of the representative fluorinated device, there is no indication of P<sub>b0</sub> center generation following NBTS. This observation suggests that the incorporation of fluorine can selectively passivate P<sub>b0</sub> precursors, that is, it is more effective at passivating the P<sub>b0</sub> precursors.

Figures 5 and 6 illustrate (weak) post-NBTS SDR traces for the two remaining somewhat differently processed fluorinated SiO<sub>2</sub> devices. Again, pre-NBTS defect spectra are below the detection limit of the spectrometer. Although the signal to noise ratios are low, the same qualitative pattern appears; a much weak SDR signal at  $g \approx 2.003$  (which is consistent with P<sub>b1</sub> center generation) and an absence of spectra expected for P<sub>b0</sub> defects. Again, the larger width of the signal may indicate the presence of nearby fluorine nuclei [17]. DC-IV measurements (not shown) for the device from Fig. 5 indicate pre-NBTS  $D_{it} = 2 \times 10^{10} \text{ cm}^{-2} \text{ eV}^{-1}$  and post-NBTS  $D_{it} = 1 \times 10^{11} \text{ cm}^{-2} \text{ eV}^{-1}$ . For the device from Fig. 6, pre-NBTS  $D_{it} = 1 \times 10^{10} \text{ cm}^{-2} \text{ eV}^{-1}$  and post-NBTS  $D_{it} = 1 \times 10^{11} \text{ cm}^{-2} \text{ eV}^{-1}$ .

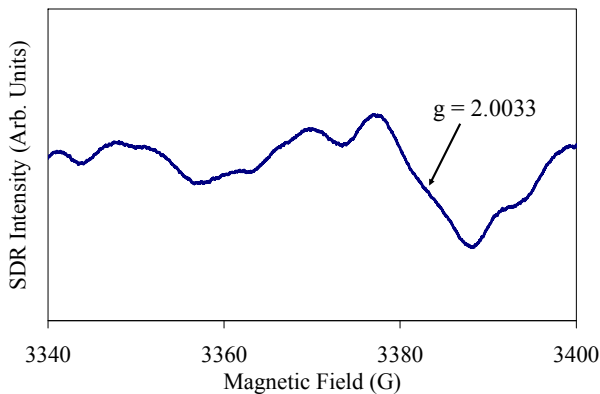


Fig. 5. Post-NBTS SDR trace of a second somewhat differently processed fluorinated device. The qualitative pattern is identical; a weak P<sub>b1</sub> signal and an absence of P<sub>b0</sub> signal.

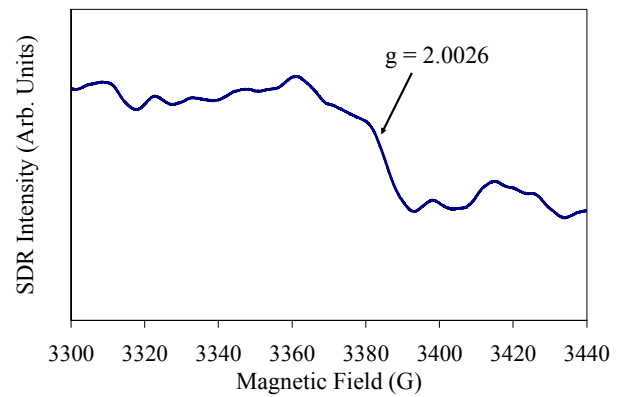


Fig. 6. Post-NBTS SDR trace of a third somewhat differently processed fluorinated device. Note the much greater breadth of the signal; this may indicate the presence of nearby fluorine nuclei.

As mentioned previously, these results indicate that fluorine incorporation can effectively passivate P<sub>b0</sub> center precursors, but less effectively passivates P<sub>b1</sub> center precursors. This would help to explain the diminished interface state generation observed in other recent reports of NBTI stressed fluorinated devices [3, 5].

P<sub>b0</sub> and P<sub>b1</sub> defects are the two variants of defect centers that dominate interface trapping at (100) Si/SiO<sub>2</sub> boundaries and are responsible for a wide range of MOS instability and performance issues [12, 13]. These defects are apparently responsible for the commonly observed increase in  $D_{it}$  following NBTI stressing of pure SiO<sub>2</sub> devices. [11, 12] The main differences between them are in the dangling bond axis of symmetry [13, 16] and their electronic density of states (DOS) [18, 19]. A schematic illustration of P<sub>b0</sub> and P<sub>b1</sub> DOS is provided in figure 6.

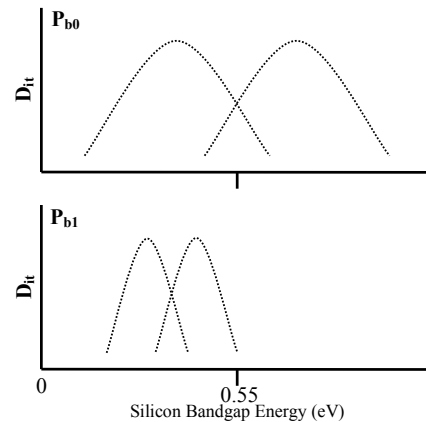


Figure 7: Schematic Illustration of P<sub>b0</sub> (top) and P<sub>b1</sub> (bottom) density of states. P<sub>b0</sub> and P<sub>b1</sub> are the dominating interface states in pure Si/SiO<sub>2</sub> MOS devices.

P<sub>b0</sub> centers have a broadly peaked DOS centered about midgap with an electron correlation energy of about 0.7eV [18]. The P<sub>b1</sub> levels are much more narrowly distributed, with a DOS skewed towards the lower half of the band gap. [19] Since these defects have significantly different DOS, our results maybe useful in modeling NBTI response in fluorinated oxide devices. The narrower P<sub>b1</sub> DOS distribution will likely

result in a larger shift in threshold voltage in proportion to the total number of  $P_{b1}$  states. That is, a higher percentage of  $P_{b1}$  centers will likely be positively charged when the pMOS transistor is on. This larger effect per defect is of course more than compensated by the smaller total number of  $P_{b1}$  centers. The result also helps explain why fluorine reduces NBTI damage in pure  $\text{SiO}_2$  devices, but not in some nitrided devices; in nitrided devices, NBTI is not dominated by  $P_b$  centers [12].

Our results may also help to explain fluorine's role in reducing the effects of hot carrier damage and improving radiation hardness. Nishioka et al. [7] and Wright et al. [8] examined the effects of fluorine on hot electron response in fluorinated MOS devices. Both studies show that fluorine incorporation leads to a more robust interface in which interface state generation is reduced compared to hot electron stressed pure  $\text{SiO}_2$  devices. They suggest that the stronger Si-F bond (compared to Si-H) or bond strain relief may be responsible for the improved interface response. Wang et al. [9] and da Silva et al. [10] showed that fluorine incorporation can improve the radiation hardness of  $\text{SiO}_2$  MOS devices resulting in a reduced interface state density following irradiation. Again, the authors argue that the stronger Si-F bond may be responsible for the improved radiation hardness. Our results clearly indicate that fluorine more effectively passivates  $P_{b0}$  centers but is less effective at passivating  $P_{b1}$  centers in NBTI stressed devices. It is very likely that a similar phenomena occurs in hot carrier stressed and irradiated devices resulting in a more robust interface. As has been noted in some of the earlier fluorine literature, these results make sense in terms of the relative strengths of Si-H and Si-F bond energies. Pauling estimated the strength of the Si-H bond to be approximately 295 KJ mole<sup>-1</sup> and the strength of the Si-F bond to be much larger, 510 KJ mole<sup>-1</sup> [20].

#### IV. CONCLUSIONS

The incorporation of fluorine in the  $\text{SiO}_2$  gate dielectric can diminish NBTI degradation [3, 5]. Our results indicate why this is so: fluorine incorporation in the  $\text{SiO}_2$  effectively passivates  $P_{b0}$  precursors and somewhat less effectively passivates  $P_{b1}$  precursors. Thus,  $P_{b1}$  centers dominate the resulting NBTI induced defect spectra. Our results also suggest that fluorine nuclei may be present near these defects.

#### ACKNOWLEDGMENTS

Work at Penn State was supported by Texas Instruments through Semiconductor Research Corporation custom funding.

#### REFERENCES

- [1] M.A. Alam and S. Mahapatra, "A comprehensive model of pMOS NBTI degradation", *Microelectron. Reliab.*, vol. 45, pp. 71-81, 2005.
- [2] S. Chakravarthi, A.T. Krishnan, V. Reddy, C.F. Machala, and S. Krishnan, "A comprehensive framework for predictive modeling of NBTI", *IEEE Int. Reliability Phys. Symp.*, pp. 273-282, 2004.
- [3] T.B. Hook, et al., "The effects of F on parametrics and reliability in a 0.18um 3.5/6.8 nm dual gate oxide CMOS technology", *IEEE Trans. Electron Devices*, vol. 48, pp. 1346-1353, 2001.
- [4] D.K. Schroder and J.A. Babcock, "NBTI: Road to cross in deep submicron Si semiconductor manufacturing", *J. Appl. Phys.*, vol. 94, pp. 1-18, 2003.
- [5] C.H. Liu, et al., "Mechanism and process dependence of NBTI for pMOSFETs with ultrathin gate dielectrics", *IEEE IEDM Tech. Dig.*, vol. pp. 861-864, 2001.
- [6] P.J. Wright and K.C. Saraswat, "The effect of F in  $\text{SiO}_2$  gate dielectrics", *IEEE Trans. Electron Devices*, vol. 36, pp. 879-889, 1989.
- [7] Y. Nishioka, E.F. Dasilva, Y. Wang, and T.P. Ma, "Dramatic improvement of hot-electron-induced interface degradation in MOS structures containing F or Cl in  $\text{SiO}_2$ ", *IEEE Elec. Dev. Lett.*, vol. 9, pp. 38-40, 1988.
- [8] P.J. Wright, N. Kasai, S. Inoue, and K.C. Saraswat, "Hot-electron immunity of  $\text{SiO}_2$  dielectrics with F incorporation", *IEEE Elec. Dev. Lett.*, vol. 10, pp. 347, 1989.
- [9] X.W. Wang and T.P. Ma, "Passivation of (111) Si/ $\text{SiO}_2$  interface by F", *Appl. Phys. Lett.*, vol. 60, pp. 2634-2636, 1992.
- [10] E.F. da Silva, Y. Nishioka, and T.P. Ma, "Radiation response of MOS capacitors containing fluorinated oxides", *IEEE Trans. Nucl. Sci.*, vol. 34, pp. 1190, 1987.
- [11] S. Fujieda, et al., "Interface defects responsible for NBTI in plasma-nitrided SiON/Si(100) systems", *Appl. Phys. Lett.*, vol. 82, pp. 3677-3679, 2003.
- [12] J.P. Campbell, P.M. Lenahan, C.J. Cochrane, A.T. Krishnan, and S. Krishnan, "Atomic-scale defects involved in NBTI", *IEEE Trans. Dev. Mater. Reliab.*, vol. 7, pp. 540-557, 2007.
- [13] P.M. Lenahan and J.F. Conley, "What can electron paramagnetic resonance tell us about the Si/ $\text{SiO}_2$  system?" *J. Vac. Sci. Technol., B*, vol. 16, pp. 2134-2153, 1998.
- [14] D.J. Fitzgerald and A.S. Grove, "Surface recombination in semiconductors", *Surf. Sci.*, vol. 9, pp. 347-369, 1968.
- [15] J.P. Campbell, P.M. Lenahan, A.T. Krishnan, and S. Krishnan, "Observations of NBTI-induced atomic-scale defects", *IEEE Trans. Dev. Mater. Reliab.*, vol. 6, pp. 117-122, 2006.
- [16] K.L. Brower, "Structural features at the Si/ $\text{SiO}_2$  interface", *Z. Phys. Chem.*, vol. 151, pp. 177-189, 1987.
- [17] J.A. Weil, J.R. Bolton, and J.E. Wertz, "Electron Paramagnetic Resonance". New York, NY: Wiley, 1994.
- [18] E.H. Poindexter, et al., "Electronic traps and  $P_b$  centers at the Si/ $\text{SiO}_2$  interface - band gap energy distribution", *J. Appl. Phys.*, vol. 56, pp. 2844-2849, 1984.
- [19] J.P. Campbell and P.M. Lenahan, "Density of states of  $P_{b1}$  Si/ $\text{SiO}_2$  interface trap centers", *Appl. Phys. Lett.*, vol. 80, pp. 1945-1947, 2002.
- [20] L. Pauling, "Appendix VIII of General Chemistry". New York: Dover, 1998.